ADVANCED MATERIALS INTERFACES
www.advmatinterfaces.de

Sequential Use of Orthogonal Self-Assembled Monolayers for Area-Selective Atomic Layer Deposition of Dielectric on Metal

*Tzu-Ling Liu, Maggy Harake, and Stacey F. Bent**

Although there have been several demonstrations of area-selective atomic layer deposition (AS-ALD) of dielectric on dielectric in metal/dielectric patterns, the reverse process of selective dielectric on metal (DoM) is not as well developed due to the challenge of inhibiting only the dielectrics. Unavoidable native oxide formation on metals tends to lead to similar surface chemical properties between metal and dielectric substrates, decreasing the selectivity in inhibitor adsorption. Hence, to achieve DoM, preventing unwanted inhibitor adsorption on metals is critical. This study demonstrates a two-step strategy of first applying a dodecanethiol (DDT) self-assembled monolayer (SAM) on a Cu/SiO_2 pattern to protect the Cu surfaces from subsequent deposition of an octadecyltrimethoxysilane (OTMS) inhibitor, which then selectively forms an OTMS SAM on SiO_2. It is further shown that by removing the DDT protector with thermal treatment before AS-ALD, subsequent ALD growth on Cu is not affected while ALD remains blocked on the OTMS-covered SiO_2 regions. Using this strategy, DoM is demonstrated with selectivity above 0.9 after 5.6 nm of ZnO and 1.5 nm of Al_2O_3 ALD. This work presents a new approach to expand the material systems available to AS-ALD which may help enable more applications in microelectronics, optoelectronics, and energy.

1. Introduction

Currently, manufacturing processes in the microelectronics industry are based on top-down approaches, requiring multiple steps such as lithography, deposition, and etching to fabricate patterned structures. However, a number of challenges, including alignment between the adjacent layers as well as increasing costs of lithography due to semiconductor device scaling, have driven research in the direction of developing more precise and robust processing methods.[1,2] Area-selective atomic layer deposition (AS-ALD), which provides a bottom-up approach to fabricate patterned structures, has been considered a prospective solution to overcome some of the challenges that are present in current semiconductor manufacturing.[3–6]

One common approach to accomplish AS-ALD uses self-assembled monolayers (SAMs) as the inhibitors to preferentially block ALD on one surface material over another.[7–14] SAMs are organic molecules that consist of a headgroup (also known as an anchoring group), which binds to the substrate surface, a backbone, which is involved in the self-assembly process via van der Waals interactions, and a tail functional group, which influences the final surface property after SAM formation. By choosing a headgroup of the SAM molecules that only reacts with a specific surface, selective SAM formation can be achieved. For example, alkanethiols and alkylphosphonic acids have been shown to form SAM structures on metal substrates but not on SiO_2.[15–21] By using these two SAM molecules as inhibitors for ALD on metal surfaces, there have been several successful demonstrations of selective deposition of both dielectric films (dielectric-on-dielectric, or DoD) and metal films (metal-on-dielectric, MoD) on the dielectric regions of metal/dielectric patterns.[7–12,22,23]

However, doing the reverse pattern transfer, i.e., selective deposition of dielectric on metal regions (DoM) while preventing ALD growth on dielectric areas, is still not well-developed because of the difficulty in achieving selective application of the inhibitor on dielectric surfaces but not on metal surfaces. For example, organosilanes, a common and effective inhibitor choice for dielectric surfaces, can also adsorb undesirably on the metal regions when there is native metal oxide present on the surface,[24–28] which is usually hard to avoid. Hence, developing an approach to protect the metal surfaces against adsorption of the inhibitor may be key to achieving AS-ALD on metals over dielectrics.

T.-L. Liu
Department of Materials Science and Engineering
Stanford University
Stanford, CA 94305, USA
M. Harake, S. F. Bent
Department of Chemical Engineering
Stanford University
Stanford, CA 94305, USA
E-mail: sbent@stanford.edu

The ORCID identification number(s) for the author(s) of this article can be found under https://doi.org/10.1002/admi.202202134.

DOI: 10.1002/admi.202202134

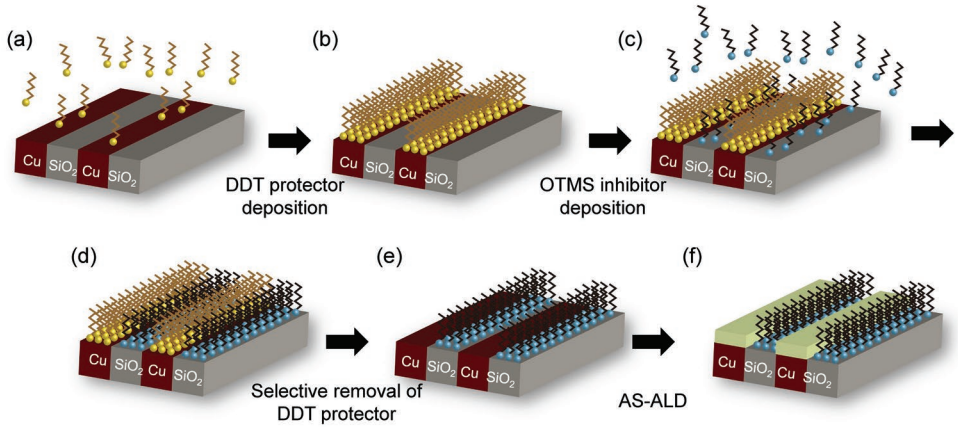

Figure 1. Schematic illustration of the process flow used for achieving selective dielectric on metal (DoM) deposition in this study.

In this work, we introduce a two-step strategy to achieve selective deposition of DoM surfaces on metal/dielectric patterns by use of two different SAMs with nearly orthogonal surface chemistry, i.e., one SAM preferentially adsorbs on the metal and the other primarily adsorbs on the dielectric. We first use alkanethiols as a protector of the metal surfaces against any unwanted adsorption of organosilane inhibitor, followed by application of the organosilanes which then selectively attach to the dielectric regions and inhibit subsequent ALD. We show that by forming a dodecanethiol (DDT) protective layer on Cu prior to octadecyltrimethoxysilane (OTMS) inhibitor exposure, the undesired adsorption of OTMS on Cu can be prevented, leaving OTMS to form a well-packed SAM structure only on SiO_2. We then conduct ALD blocking tests using both ZnO and Al_2O_3 ALD as model systems after applying a thermal step to selectively remove the DDT protector from Cu. With Cu as the growth surface and SiO_2 as the nongrowth surface, selectivity above 0.9 can be maintained after 35 cycles of ZnO ALD (5.6 nm of ZnO on reference native SiO_2-covered Si) and 15 cycles of Al_2O_3 ALD (1.5 nm of Al_2O_3 on reference native SiO_2-covered Si), respectively, using this sequential SAM process. Finally, selective deposition of DoM is demonstrated on Cu/SiO_2 and Cu/low-*k* patterns using the combined OTMS inhibitor and DDT protector. Our study helps expand the selective deposition toolbox to enable more potential applications for AS-ALD in next generation electronic device manufacturing.

2. Results and Discussion

To achieve AS-ALD on Cu (the intended growth surface for ALD) over SiO_2 (the nongrowth surface), selective inhibitor formation only on SiO_2 surfaces is required. However, while organosilane inhibitors largely adsorb on SiO_2, some adsorption by the organosilanes can also occur on Cu (vide supra),[28] leading to greatly reduced selectivity in AS-ALD. To prevent the adsorption of OTMS on Cu, DDT deposition is first performed to generate a DDT SAM on Cu surfaces, as illustrated schematically in **Figure 1**b. Following DDT treatment, a high water contact angle (WCA) value of 105° is measured on Cu substrates (Cu-DDT) as shown in **Table 1**, indicating the successful formation of a DDT SAM layer,[32–34] which we hypothesize will protect Cu from subsequent OTMS adsorption. On the other hand, a low WCA value of 19 ± 3° (Table 1) is measured on SiO_2 even after DDT treatment (SiO_2-DDT) suggesting that no DDT adsorption occurs on the SiO_2 surface, consistent with previous reports.[8,12,33,34] Therefore, the subsequent deposition of the OTMS inhibitor after DDT exposure should not be impacted on SiO_2.

For OTMS to inhibit ALD on SiO_2, it needs to form a well-packed SAM. One key factor that influences the formation of a well-packed organosilane SAM is the amount of water present in the deposition system. Without enough water, the hydrolysis and condensation reactions of organosilane molecules cannot be promoted, leading to the formation of a partial SAM layer.[35] On the other hand, if there is too much water in the system, organosilane molecules can form large polymerized aggregates in solution before adsorbing onto the surface, leading to nonuniform and rough films.[24,35] In either case of nonoptimal water concentration, the organosilane layer that forms may possess insufficient blocking ability. Hence, we studied the role of water concentration on the quality of the OTMS SAM. We compared the effect of using anhydrous solvent versus standard solvent on OTMS SAM formation. **Table 2** shows the WCA and the thickness of the OTMS layer on a SiO_2 substrate after it was first treated with DDT then exposed to OTMS in the two different solvents. On SiO_2 substrates treated by the DDT protector followed by OTMS inhibitor (given the notation SiO_2-DDT/OTMS), the WCA results are the same within the uncertainty of the measurement between the anhydrous and standard toluene solvent; however, the thicknesses of the OTMS layer does differ between the two solvents. Using standard toluene results in a thicker OTMS layer that is closer to the ideal length of an 18C alkyl chain (27–28 Å),[17,24,36] suggesting a better packed SAM is

Table 1. WCA measurements on different substrates after 1st step of DDT protector deposition.

1st step: DDT protector deposition		
	SiO_2-DDT	Cu-DDT
WCA (°)	19 ± 3	105

WCA data of SiO_2-DDT are shown as mean ± 1 standard deviation with sample size = 3.

Table 2. WCA and ellipsometric thickness measurements on different substrates after 2nd step of OTMS SAM deposition in both standard and anhydrous toluene solvents.

2nd step: OTMS inhibitor deposition						
	SiO_2-DDT/OTMS		Cu-DDT/OTMS		Cu-OTMS	
Solvent	Anhydrous	Standard	Anhydrous	Standard	Anhydrous	Standard
WCA (*)	109 ± 1	111 ± 2	106 ± 2	101 ± 4	81 ± 37	95 ± 14
Thickness [Å]	23.4 ± 2.0	28.1 ± 0.6	–	–	–	–

Data are shown as mean ± 1 standard deviation with sample size = 3. The statistical significance of the difference between the OTMS thickness on SiO2-DDT/OTMS using different toluene solvents is compared using a two-sample *t*-test. The calculated *p*-value (two-tailed) = 0.005.

formed.[37] Consequently, our subsequent studies used standard toluene as the solvent for OTMS SAM formation.

After OTMS was demonstrated to form a well-packed SAM structure on SiO_2 following solvent optimization, the effectiveness of using the DDT protector to prevent OTMS adsorption on Cu was investigated. Table 2 shows the WCA on Cu substrates with and without the DDT protector after OTMS deposition (Cu-DDT/OTMS and Cu-OTMS, respectively) for both solvents. First we discuss the results of the OTMS behavior on bare Cu substrates (i.e., without DDT protector). WCA values of 81 ± 37° and 95 ± 14° are obtained on Cu-OTMS using anhydrous and standard toluene, respectively. By comparison to the WCA on a cleaned reference Cu sample (41°), the increase in WCA on Cu-OTMS confirms that some undesired adsorption of OTMS molecules does occur on the Cu surface. These adsorbed OTMS molecules can act to inhibit ALD on Cu during the subsequent AS-ALD process and negatively affect the selectivity. On the other hand, the behavior is different on the DDT-protected Cu surfaces. Measurements on Cu-DDT/OTMS using both solvents show WCAs similar to those on Cu-DDT before OTMS deposition. This result could imply that the DDT SAM remains relatively intact and successfully protects the Cu surface from OTMS adsorption. However, these data alone do not rule out a second possibility, which is that the DDT protector does allow some undesired OTMS molecules to adsorb on the surface, which would also result in a high WCA value. To distinguish between the two possibilities, additional analysis is performed, as discussed below.

X-ray photoelectron spectroscopy (XPS) fine scans over the Si 2p region were conducted on Cu-DDT/OTMS and compared with those on Cu-OTMS to probe whether the DDT protector helps prevent OTMS adsorption on Cu. Because Si is a component only of the OTMS molecules, the presence of Si signal can be used to probe whether OTMS is present at the surface. The results of the study are shown in **Figure 2**. The figure shows that a Si 2p peak at 102.2 eV is observed on Cu-OTMS,[28] indicating some undesired adsorption of OTMS on Cu, consistent with the WCA results in Table 2. In contrast, no Si signal is detected on Cu-DDT/OTMS, indicating the effectiveness of the DDT protector in preventing undesired OTMS adsorption on Cu. From the absence of Si signal on Cu-DDT/OTMS, it can be concluded that the high WCA values in Table 2 are due to the DDT SAM rather than OTMS.

After successfully demonstrating the orthogonal SAM formation, i.e., the selective deposition of OTMS inhibitors only on SiO_2 facilitated by the DDT protector only on the Cu surface, ALD blocking tests were conducted on all the samples. To achieve maximum selectivity between Cu and SiO_2, it is necessary to remove the DDT protector from the Cu before carrying out ALD. Otherwise, the DDT protector on Cu would also act as an ALD inhibitor[12,32–34] and affect the final selectivity. Because the temperature stability of alkanethiols (<160 °C) is much lower than that of organosilanes (<450 °C),[38–41] the DDT layer on Cu surfaces can be selectively desorbed or decomposed without causing damage to the OTMS inhibitor on SiO_2 simply by performing ALD at an appropriate temperature. To identify the optimal ALD temperature, 15 cycles of ZnO ALD were conducted on reference Cu and Cu-DDT/OTMS at both 150 °C and 200 °C with a 15 min waiting time under vacuum prior to introducing ALD precursors; both temperatures are within the reported ALD temperature window for ZnO.[42] On reference Cu, XPS atomic compositional analysis shows Zn/(Zn + Cu) ratios of 0.88 and 0.85 ± 0.12 at ALD temperatures of 150 °C and 200 °C, respectively; however, on Cu-DDT/OTMS, the respective ratios are 0.47 and 0.80 ± 0.12 (**Table 3**). By comparing the Zn/(Zn + Cu) ratio on reference Cu and Cu-DDT/OTMS, the results indicate a nucleation delay of ZnO on Cu-DDT/OTMS at 150 °C, suggesting that some DDT protectors remain on Cu and inhibit the ZnO ALD

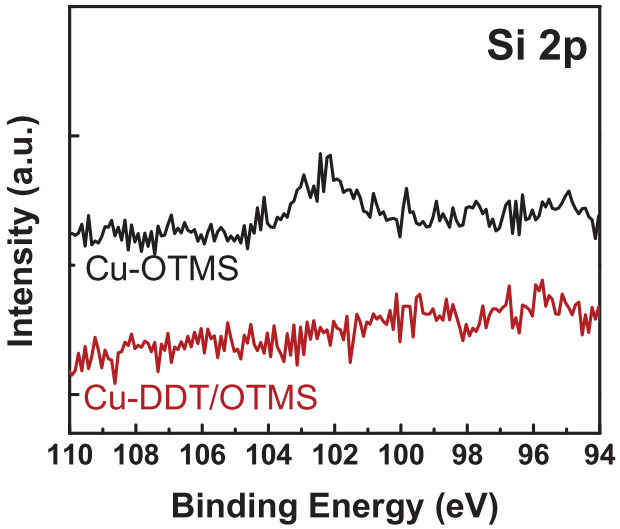

Figure 2. XPS fine Si 2p scans of Cu substrates with and without DDT protector after OTMS SAM deposition.

Table 3. Zn/(Zn + Cu) ratio on Cu samples after 15 cycles ZnO ALD at different ALD temperatures.

Zn/(Zn + Cu) ratio from XPS		
	Cu	Cu-DDT/OTMS
150 °C	0.88	0.47
200 °C	0.85 ± 0.12	0.80 ± 0.12

Data of 200 °C are shown as mean ± 1 standard deviation with sample size = 3. The statistical significance of the difference between the data points of reference Cu and Cu-DDT/OTMS after ALD at 200 °C is compared using a two-sample *t*-test. The calculated *p*-value (two-tailed) = 0.52.

at that temperature. In contrast, the similar Zn/(Zn + Cu) ratios on reference Cu and Cu-DDT/OTMS at an ALD temperature of 200 °C indicate that at 200 °C the DDT protector on Cu is removed and does not participate in blocking ALD. We note that studies have shown a layer of chemisorbed sulfur remaining on the metal surface after the thermal desorption of alkanethiols.[43] Interestingly, chemisorbed sulfur does not seem to affect ALD growth according to the data in Table 3. WCA measurement was also conducted on Cu-DDT/OTMS after 15 min of annealing under vacuum at 200 °C. The low WCA measured (35°) confirms the removal of the DDT SAM. Hence, the ALD blocking tests in this study were performed at

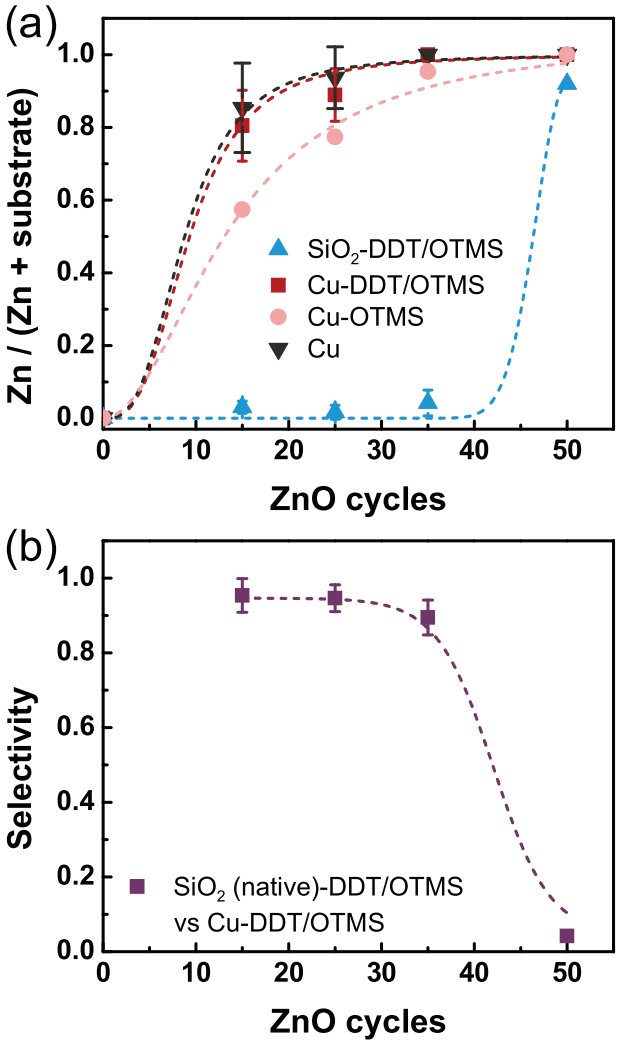

Figure 3. a) Atomic composition ratios from XPS analysis of SiO_2-DDT/OTMS, Cu-DDT/OTMS, Cu-OTMS, and reference Cu substrates with increasing cycles of ZnO ALD at 200 °C. b) Selectivity of ZnO ALD between SiO_2-DDT/OTMS (nongrowth surface) and Cu-DDT/OTMS (growth surface) extracted from the data in (a). The dashed curves serve as guides to the eye. The data points with error bars were repeated three times each, and are shown as mean ± 1 standard deviation. The statistical significances of the difference in the blocking results after 15 cycles ALD between reference Cu and Cu-DDT/OTMS and between SiO_2-DDT/OTMS and Cu-DDT/OTMS are compared using a two-sample *t*-test. The calculated *p*-value (two-tailed) = 0.52 and 0.00002, respectively.

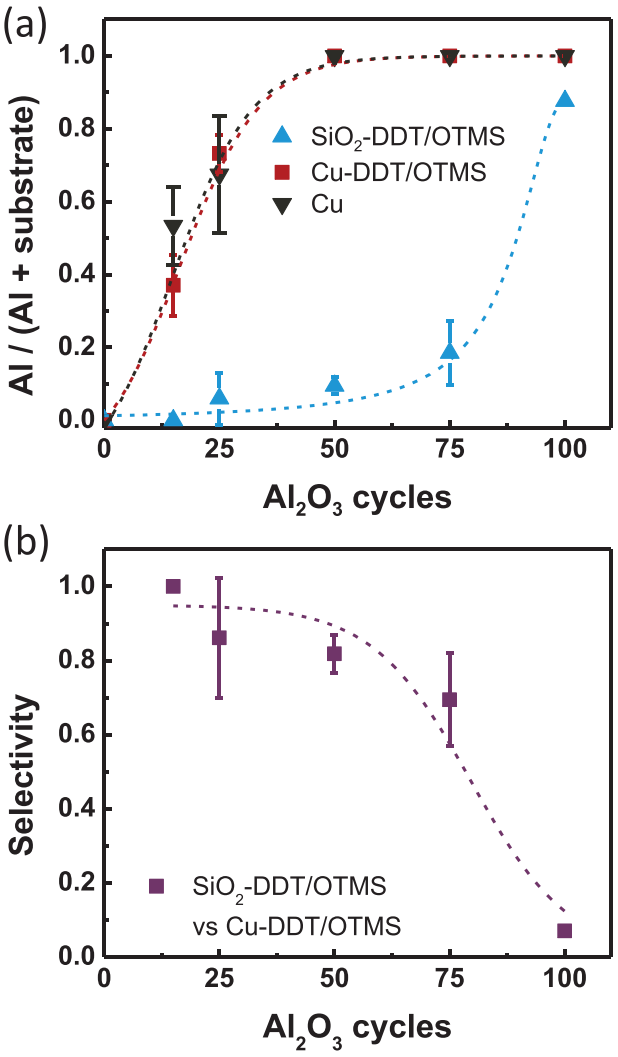

Figure 4. a) Atomic composition ratios from XPS analysis of reference Cu, SiO_2-DDT/OTMS, and Cu-DDT/OTMS substrates with increasing cycles of Al_2O_3 ALD. b) Selectivity of Al_2O_3 ALD between SiO_2-DDT/OTMS (nongrowth surface) and Cu-DDT/OTMS (growth surface) extracted from the data in (a). The dashed curves serve as guides to the eye. The data points with error bars were repeated three times, and are shown as mean ± 1 standard deviation. The statistical significances of the difference in the blocking results after 15 cycles ALD between reference Cu and Cu-DDT/OTMS and between SiO_2-DDT/OTMS and Cu-DDT/OTMS are compared using a two-sample *t*-test. The calculated *p*-value (two-tailed) = 0.11 and 0.002, respectively.

200 °C after 15 min holding time in the ALD reactor to ensure complete DDT removal prior to the ALD process.

To test the blocking ability of OTMS inhibitors against ALD, both ZnO and Al_2O_3 ALD were selected as model ALD systems in this work. **Figure 3**a shows the Zn atomic ratio on three different Cu samples and on SiO_2-DDT/OTMS after increasing cycle numbers of ZnO ALD. The results reveal that approximately 25–35 cycles of ZnO ALD can be blocked on SiO_2-DDT/OTMS. In addition, similar Zn/(Zn + Cu) ratios are obtained on reference Cu and Cu-DDT/OTMS, which indicates that there is no ZnO nucleation delay on Cu-DDT/OTMS (the growth surface for ALD). This result is consistent with the previous observation that no OTMS adsorption occurs on Cu if the DDT protector is used (Figure 2) and that the DDT protector can be removed by operating ALD at a sufficiently high temperature. On the other hand, the lower Zn/(Zn + Cu) ratio on Cu-OTMS compared to reference Cu suggests that ZnO ALD is partly inhibited when the DDT protector step is skipped, a result that can be attributed to the undesired adsorption of OTMS inhibitor on Cu, as observed by XPS (Figure 2). The ALD selectivity between Cu-DDT/OTMS (growth surface) and SiO_2-DDT/OTMS (nongrowth surface) is then calculated with the following equation.[44,45]

$$S = \frac{R_{gs} - R_{ns}}{R_{gs} + R_{ns}} \quad (1)$$

where R represents the relevant atomic composition ratio. Specifically, R_{gs} represents the atomic composition ratio on the Cu growth surface (gs), i.e., Zn/(Zn + Cu) or Al/(Al + Cu), and R_{ns} represents the atomic ratio on the SiO_2 nongrowth surface (ns), i.e., Zn/(Zn + Si) or Al/(Al + Si), respectively. Here, selectivity (S) ranges from 0 (no selectivity) to 1 (perfect selectivity). From the calculated selectivity values in Figure 3b, it is seen that $S > 0.9$ can be maintained up to at least 35 cycles of ZnO ALD. These results confirm that with our strategy of applying a DDT protector on Cu prior to OTMS deposition, selective deposition of DoM can be achieved.

Figure 4 shows the results of the dual blocking process applied to Al_2O_3 ALD and the corresponding calculated selectivity. Similar to ZnO, no significant difference in Al_2O_3 growth is observed between Cu-DDT/OTMS and reference Cu. For the nongrowth surface, i.e., SiO_2-DDT/OTMS, about 15–25 cycles of Al_2O_3 can be delayed by the OTMS inhibitor before significant nucleation begins to occur. From the calculated selectivity values in Figure 4b, it can be seen that $S > 0.9$ is obtained for 15 cycles of Al_2O_3 but drops at higher cycle numbers. It is clear from a comparison of the ZnO and Al_2O_3 blocking results that the ZnO ALD is easier to block, agreeing with previous studies,[34,44,46] suggesting the importance of the ALD precursor in AS-ALD.[47]

Finally, AS-ALD of DoM is demonstrated on metal/dielectric patterns. **Figure 5**a–c show the scanning electron microscope (SEM) image and the Auger electron spectroscopy (AES) Si and Cu elemental mappings of a Cu/SiO_2 pattern, revealing the surface composition of the starting pattern. Figure 5d,e show the AES Zn mappings of the Cu/SiO_2 patterned substrates after ZnO ALD for two cases: in (d), the experiment was performed without the DDT protector step, and in (e) the experiment was performed with the DDT protector step, followed in both cases by OTMS inhibitor deposition and then 25 cycles of ZnO ALD at 200 °C. The results of both experiments show selective deposition of ZnO primarily on the Cu regions of the patterns. However, the relatively nonuniform intensity of Zn signal on the Cu/SiO_2 pattern without the DDT protector (Figure 5d) suggests that ZnO has nucleated poorly (nucleation delay) on the Cu growth surface, presumably because of residual OTMS present at that surface. The Zn line scans in Figure 5f further confirm the observations in Figure 5d,e. Namely, the sample that received the DDT protector shows sharp differentiation of the Zn signal between the Cu and SiO_2 regions of the pattern, whereas the sample without DDT shows highly variable signal

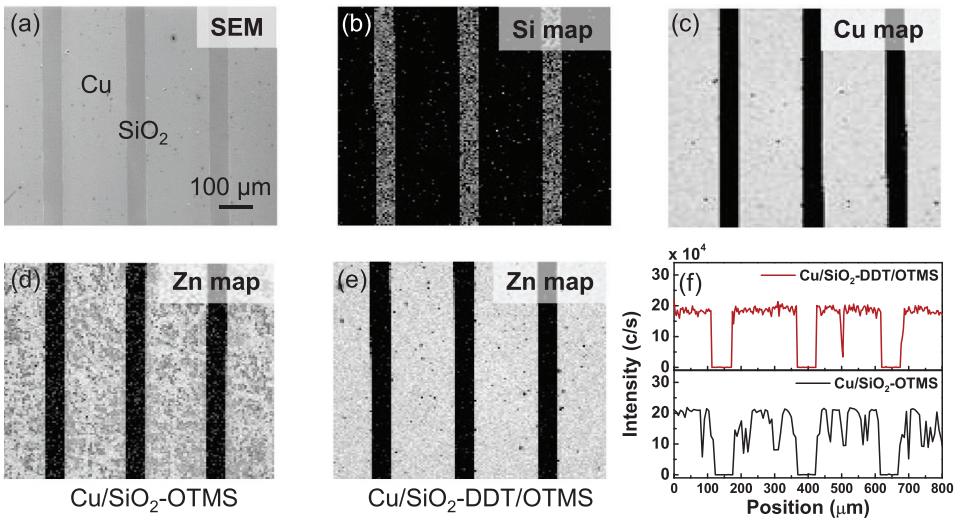

Figure 5. a) SEM image and AES b) Si and c) Cu elemental mappings of a Cu/SiO_2 pattern before SAM treatment or ALD. AES Zn elemental mappings of Cu/SiO_2 patterns d) without and e) with DDT treatment followed by OTMS after 25 cycles ZnO ALD, and f) the corresponding AES Zn line scans. Images (b–e) are at the same scale as that in (a).

on the Cu regions of the pattern. The results confirm the benefit of using the DDT protector on Cu surfaces before applying the OTMS inhibitor. From the AES line scans, the selectivity can be extracted using the ratio of $(I_{gs} - I_{ns})/(I_{gs} + I_{ns})$, where I_{gs} and I_{ns} represent the averaged intensity counts from the AES line scans of the ALD materials on the Cu growth surface and on the SiO_2 nongrowth surface, respectively. A selectivity = 0.99 is obtained on patterned Cu/SiO_2-DDT/OTMS samples after 25 cycles of ZnO ALD.

Similar results for selective Al_2O_3 ALD are also obtained on Cu/SiO_2 patterns treated with the DDT protector followed by OTMS deposition. **Figure 6**a,b show the SEM image and the AES Al elemental map of a patterned Cu/SiO_2-DDT/OTMS sample after 50 cycles Al_2O_3 ALD. The result shows that Al_2O_3 is selectively grown on Cu areas, with a selectivity = 0.99 calculated from the AES Al line scan data (Figure 6c). We note that the values of selectivity calculated from the AES measurements differ from those calculated from XPS for the same number of ZnO and Al_2O_3 ALD cycles, with the AES-obtained selectivities systematically higher. We hypothesize that this difference arises from the different spot sizes of XPS and AES, which are 200 µm for XPS and 10 nm for scanning AES. Because of the small spot size in the AES measurement, only a very small portion of the area in one pixel (10×10 nm^2 in 5×6 µm^2) is detected during collection of each point that comprises the line scan data. Since the ALD materials form discontinuous nuclei on the SAM surfaces,[48] it is possible that the scanning Auger measurement misses ALD nuclei on the nongrowth surface during the scan, which could lead to better calculated selectivity.

In addition to Cu/SiO_2 patterns, AS-ALD of DoM is demonstrated using the same two step protection-plus-inhibition approach on Cu/SiCOH low-*k* dielectric patterns, given the importance of the Cu/SiCOH low-*k* materials system in modern backend semiconductor processeses. Since the surface properties of the SiCOH low-*k* dielectric material are similar to that of SiO_2, the ALD inhibition process is expected to apply to Cu/SiCOH low-*k* patterns as well. Here, we also investigated patterns with smaller feature sizes (≈500 nm versus 50 µm). **Figure 7** shows the SEM image and AES elemental maps, demonstrating successful selective deposition of ZnO and Al_2O_3 on the Cu regions of Cu/SiCOH low-*k* dielectric patterns. Selectivity values calculated from the AES line scan data (Figure S2, Supporting Information) show that $S = 0.93$ and 0.86 are achieved after 25 cycles of ZnO and 50 cycles of Al_2O_3, respectively. Comparing the AES results in Figures 5–7, it is evident that slightly poorer selectivity is obtained on Cu/SiCOH low-*k* dielectric patterns than on Cu/SiO_2 patterns after ALD blocking. We postulate that this difference is due to the different surface properties of the SiO_2 and SiCOH low-*k* dielectric substrate; the SiCOH low-*k* dielectrics exhibits a more hydrophobic nature than SiO_2,[49] leading to the formation of a slightly less well-packed OTMS SAM structure.

3. Conclusion

To achieve AS-ALD of DoM, a main challenge of selective inhibitor formation on dielectric substrates over metal substrates is overcome by the protocol introduced in this study.

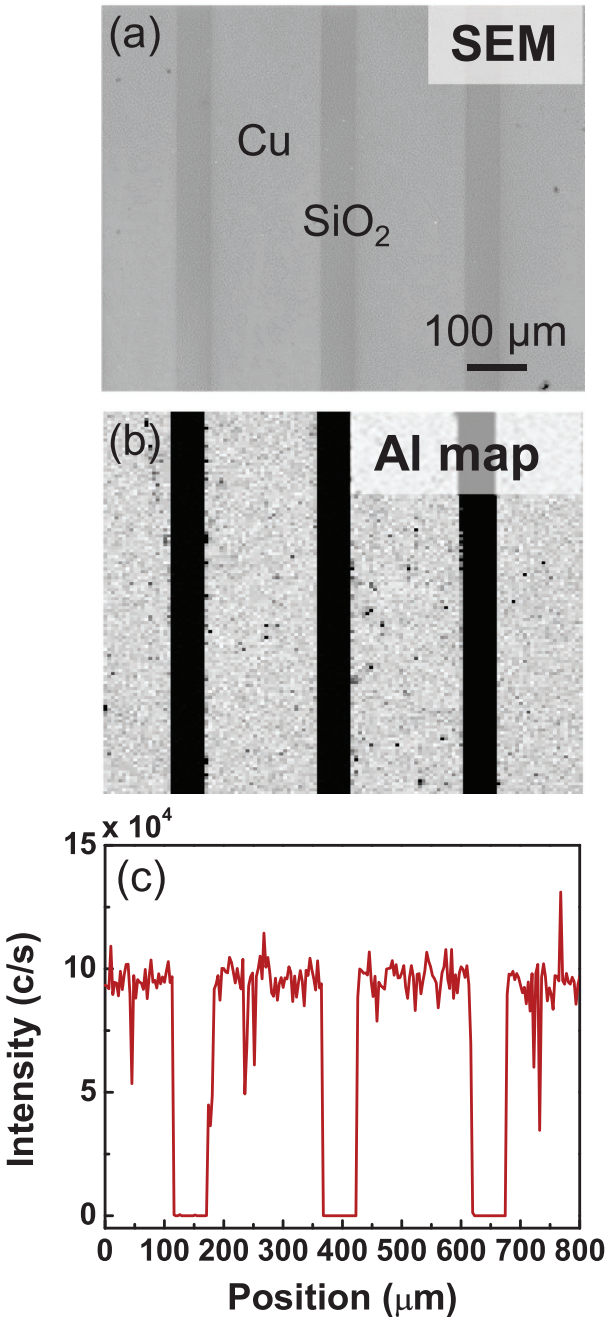

Figure 6. a) SEM image and Al elemental b) map and c) line scan from AES of Cu/SiO_2 patterns treated by DDT followed by OTMS after 50 cycles of Al_2O_3 ALD. Image (b) is at the same scale as that in (a).

AS-ALD of DoM is demonstrated by introducing a two-step blocking strategy in which a DDT protector first adsorbs selectively on Cu followed by exposure to an OTMS inhibitor which forms a SAM selectively on SiO_2 surfaces. We show DDT can effectively protect Cu surfaces from adventitious OTMS deposition. In addition, due to the different thermal stabilities between the DDT protector and OTMS inhibitor, the DDT layer on Cu can be easily removed without causing significant damage to the OTMS inhibitor. We show that DDT is

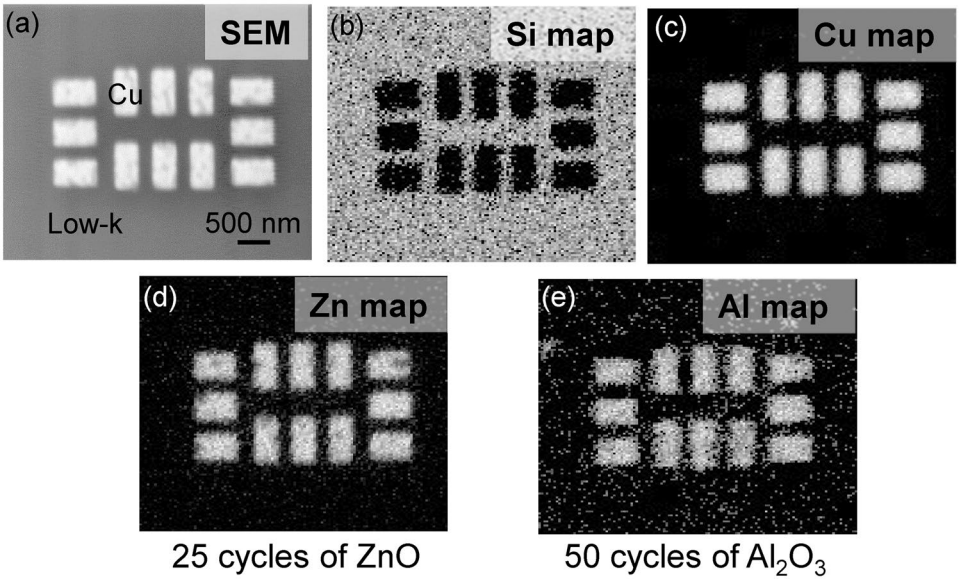

Figure 7. a) SEM image and b) Si and c) Cu elemental mappings determined by AES of a Cu/SiCOH low-*k* dielectric pattern. d) Zn and e) Al elemental mapping from AES of Cu/SiCOH low-*k* dielectric patterns treated by DDT followed by OTMS after ZnO and Al_2O_3 ALD, respectively. All images are at the same scale. Corresponding line scans are shown in Figure S2 (Supporting Information).

thermally removed from Cu surfaces at ALD process temperatures, allowing the Cu regions of a Cu/SiO_2 pattern to remain available for ALD. Measurements using the dual process show that selectivities as high as 0.99 can be achieved after 25 cycles of ZnO and 50 cycles of Al_2O_3 ALD. Finally, AS-ALD on the metal regions of metal/dielectric patterns is demonstrated on both Cu/SiO_2 and Cu/SiCOH low-*k* dielectric patterns with nm scale features. This work introduces the possibility of gaining higher selectivity by use of two different SAMs with orthogonal surface chemistry to sequentially protect different surfaces.

4. Experimental Section

Sample Preparation: Substrates of blanket Cu (i.e., unpatterned Cu), patterned Cu/SiO_2, and patterned Cu/SiCOH low-*k* dielectric with low porosity were obtained from collaborators, while blanket native SiO_2-covered Si wafers, referred as SiO_2 in this study, were purchased from WRS Materials. Blanket Cu substrates were fabricated by physical vapor deposition (PVD) followed by chemical mechanical polishing. Patterned Cu/SiO_2 and patterned Cu/SiCOH low-*k* dielectric substrates were made by lithography methods. For the patterned substrates, the Cu was deposited by PVD, the SiO_2 was deposited by thermal oxidation, and the SiCOH low-*k* dielectric was deposited by plasma enhanced chemical vapor deposition. Before SAM deposition, substrates were sonicated in ethanol for 10 min followed by 15 min of UV ozone treatment to remove surface contaminants and hydrolyze the surface. After cleaning, substrates were immersed into glacial acetic acid for 2–3 min to remove the copper oxide formed during the UV ozone cleaning.[29] Then substrates were transferred immediately into a home-built vacuum chamber for vapor DDT (>98%, Sigma-Aldrich) SAM deposition. The detailed description of the DDT chamber can be found in previous reports.[12] After introducing the substrates into the DDT chamber, it was purged with N_2 for 10 min and then pumped down to base pressure (≈2 mTorr). DDT vapor was introduced into the chamber with no observable increase of the chamber pressure, and the substrates were exposed to DDT vapor for 15 min. After the DDT deposition, the chamber was purged again with N_2 for 2–3 min to remove any unreacted DDT from the substrate. The DDT-treated substrates, which will be referred as substrate-DDT (e.g., SiO_2-DDT and Cu-DDT), were then placed in sample vials where they were immersed into a solution that contained 50×10^{-3} M OTMS (≥90%, Sigma-Aldrich) and 20×10^{-3} M acetic acid in toluene (≥99.5%, Sigma-Aldrich). The acetic acid was added to the OTMS solution to act as a catalyst to promote the OTMS SAM formation.[30,31] The sample vials were sealed by closing the vial caps and placed in a dry-air purged glovebox for 48 h. After OTMS SAM deposition, the substrates were sonicated in toluene for 3 min to remove any physisorbed OTMS from the sample surfaces. The DDT-treated samples followed by OTMS deposition will be referred to as substrate-DDT/OTMS (e.g., SiO_2-DDT/OTMS and Cu-DDT/OTMS) throughout this report.

ALD Blocking: The blocking experiments were performed in a GemStar 6 reactor (Arradiance Inc.). Diethylzinc (DEZ, Sigma-Aldrich) and trimethylaluminum (TMA, 97%, Sigma-Aldrich) were used as the precursors for ZnO and Al_2O_3 ALD, respectively. Water was used as the counter-reactant for both ALD processes. All precursors were kept at room temperature and dosed into the reactor with 30 ms pulse followed by 10 s of N_2 purge. Both ALD processes were conducted at 200 °C with a 15 min waiting time under vacuum prior to introducing ALD precursors. The growth rate (growth per cycle, GPC) of ZnO and Al_2O_3 ALD on reference Si wafers were 1.6 and 1.0 Å cyc^{-1}, respectively (Figure S1, Supporting Information).

Sample Characterization: WCA measurements were performed on a Rame-Hart 290 goniometer to characterize the hydrophobicity of SAM-covered samples. Compositional analysis was done by XPS on a PHI VersaProbe III instrument equipped with monochromatized Al Kα radiation of 1486 eV. The XPS survey scan with a step size of 1 eV per step and fine scans with a step size of 0.1 eV per step were collected with a pass energy of 224 and 55 eV, respectively. AES mappings and line scans were performed on a PHI 700 Scanning Auger Nanoprobe with beam settings 10 kV and 10 nA and pixel resolution of 128. The thicknesses of the ZnO, Al_2O_3, and OTMS SAM were measured by an alpha-SE ellipsometer (J.A. Woollam Co.)

at incident angles of 65° and 70° with a 380–900 nm wavelength range and fitted by CompleteEASE software (J.A. Woollam Co.).

Statistical Analysis: The XPS blocking data are shown as the atomic composition ratio of the deposited ZnO or Al_2O_3 ALD on the substrates, defined as Zn/(Zn + substrate) or Al/(Al + substrate). The data in Tables 1–3 and Figures 3 and 4 are expressed as mean ± standard deviation, and the sample sizes are described in the corresponding captions. The statistical method used to assess significant differences is a two-sample *t*-test, and statistical difference is defined as p-value < 0.05.

Supporting Information

Supporting Information is available from the Wiley Online Library or from the author.

Acknowledgements

Initial studies of the DDT protectors were supported by NEW LIMITS, a center in nCORE, a Semiconductor Research Corporation (SRC) program sponsored by NIST through award number 70NANB17H041. Part of this work was performed at the Stanford Nano Shared Facilities (SNSF), supported by the National Science Foundation under award ECCS-2026822. [Correction added on 14th February after initial publication: The sentence in front of Equation (1) was corrected from "The ALD selectivity between SiO_2-DDT/OTMS (growth surface) and Cu-DDT/OTMS (nongrowth surface) is then calculated with the following equation." to "The ALD selectivity between Cu-DDT/OTMS (growth surface) and SiO_2-DDT/OTMS (nongrowth surface) is then calculated with the following equation."]

Conflict of Interest

The authors declare no conflict of interest.

Data Availability Statement

The data that support the findings of this study are available from the corresponding author upon reasonable request.

Keywords

alkanethiol, area-selective deposition, dielectric on metal, organosilane

Received: September 28, 2022
Revised: November 8, 2022
Published online: December 4, 2022

[1] R. Clark, K. Tapily, K.-H. Yu, T. Hakamata, S. Consiglio, D. O'Meara, C. Wajda, J. Smith, G. Leusink, *APL Mater.* **2018**, *6*, 058203.
[2] H. Iwai, K. Kakushima, H. Wong, *Int. J. High Speed Electron. Syst.* **2006**, *16*, 43.
[3] G. N. Parsons, R. D. Clark, *Chem. Mater.* **2020**, *32*, 4920.
[4] R. W. Johnson, A. Hultqvist, S. F. Bent, *Mater. Today* **2014**, *17*, 236.
[5] H.-B.-R. Lee, S. F. Bent, *Atomic Layer Deposition of Nanostructured Materials*, Vol. 4, Wiley-VCH Verlag GmbH & Co., KGaA, Weinheim, Germany **2012**, pp. 193–225.
[6] R. Wojtecki, J. Ma, I. Cordova, N. Arellano, K. Lionti, T. Magbitang, T. G. Pattison, X. Zhao, E. Delenia, N. Lanzillo, A. E. Hess, N. F. Nathel, H. Bui, C. Rettner, G. Wallraff, P. Naulleau, *ACS Appl. Mater. Interfaces* **2021**, *13*, 9081.
[7] M. D. Sampson, J. D. Emery, M. J. Pellin, A. B. F. Martinson, *ACS Appl. Mater. Interfaces* **2017**, *9*, 33429.
[8] T.-L. Liu, S. F. Bent, *Proceedings of SPIE, Advances in Patterning Materials and Processes XXXVI*, Vol. *10960*, SPIE, Bellingham, WA **2019**, 109600O.
[9] N. P. Kobayashi, C. L. Donley, S.-Y. Wang, R. S. Williams, *J. Cryst. Growth* **2007**, *299*, 218.
[10] W. Dong, K. Zhang, Y. Zhang, T. Wei, Y. Sun, X. D. N. Chen, *Sci. Rep.* **2014**, *4*, 4458.
[11] E. Färm, M. Vehkamäki, M. Ritala, M. Leskelä, *Semicond. Sci. Technol.* **2012**, *27*, 074004.
[12] F. S. M. Hashemi, S. F. Bent, *Adv. Mater. Interfaces* **2016**, *3*, 1600464.
[13] S. S. Masango, R. A. Hackler, A. I. Henry, M. O. McAnally, G. C. Schatz, P. C. Stair, R. P. Van Duyne, *J. Phys. Chem. C* **2016**, *120*, 3822.
[14] J. R. Avila, E. J. Demarco, J. D. Emery, O. K. Farha, M. J. Pellin, J. T. Hupp, A. B. F. Martinson, *ACS Appl. Mater. Interfaces* **2014**, *6*, 11891.
[15] Y. Feng, W. Teo, K. Siow, Z. Gao, K. Tan, A. Hsieh, *J. Electrochem. Soc.* **1997**, *144*, 55.
[16] D. Y. Petrovykh, H. Kimura-Suda, A. Opdahl, L. J. Richter, M. J. Tarlov, L. J. Whitman, *Langmuir* **2006**, *22*, 2578.
[17] M. D. Porter, T. B. Bright, D. L. Allara, C. E. D. Chidsey, *J. Am. Chem. Soc.* **1987**, *109*, 3559.
[18] J. C. Love, L. A. Estroff, J. K. Kriebel, R. G. Nuzzo, G. M. Whitesides, *Chem. Rev.* **2005**, *105*, 1103.
[19] P. E. Laibinis, G. M. Whitesides, D. L. Allara, Y.-T. Tao, A. N. Parikh, R. G. Nuzzo, *J. Am. Chem. Soc.* **1991**, *113*, 7152.
[20] G. Fonder, I. Minet, C. Volcke, S. Devillers, J. Delhalle, Z. Mekhalif, *Appl. Surf. Sci.* **2011**, *257*, 6300.
[21] F. S. M. Hashemi, C. Prasittichai, S. F. Bent, *ACS Nano* **2015**, *9*, 8710.
[22] F. S. M. Hashemi, C. Prasittichai, S. F. Bent, *J. Phys. Chem. C* **2014**, *118*, 10957.
[23] C.-W. Chang, H.-H. Hsu, C.-S. Hsu, J.-T. Chen, *J. Mater. Chem. C* **2021**, *9*, 14589.
[24] Y. Wang, M. Lieberman, *Langmuir* **2003**, *19*, 1159.
[25] Z. Zhu, G. Xu, Y. An, C. He, *Colloids Surf. A* **2014**, *457*, 408.
[26] J. P. Lee, H. K. Kim, C. R. Park, G. Park, H. T. Kwak, S. M. Koo, M. M. Sung, *J. Phys. Chem. B* **2003**, *107*, 8997.
[27] S. S. Kelkar, D. Chiavetta, C. A. Wolden, *Appl. Surf. Sci.* **2013**, *282*, 291.
[28] E. Hoque, J. A. Derose, R. Houriet, P. Hoffmann, H. J. Mathieu, *Chem. Mater.* **2007**, *19*, 798.
[29] K. L. Chavez, D. W. Hess, *J. Electrochem. Soc.* **2001**, *148*, G640.
[30] W. R. Thompson, M. Cai, M. Ho, J. E. Pemberton, *Langmuir* **1997**, *13*, 2291.
[31] Y. Ito, A. A. Virkar, S. Mannsfeld, H. O. Joon, M. Toney, J. Locklin, Z. Bao, *J. Am. Chem. Soc.* **2009**, *131*, 9396.
[32] L. Lecordier, S. Herregods, S. Armini, *J. Vac. Science Technol., A* **2018**, *36*, 031605.
[33] F. S. M. Hashemi, B. R. Birchansky, S. F. Bent, *ACS Appl. Mater. Interfaces* **2016**, *8*, 33264.
[34] T.-L. Liu, K. L. Nardi, N. Draeger, D. M. Hausmann, S. F. Bent, *ACS Appl. Mater. Interfaces* **2020**, *12*, 42226.
[35] N. R. Glass, R. Tjeung, P. Chan, L. Y. Yeo, J. R. Friend, *Biomicrofluidics* **2011**, *5*, 036501.
[36] R. Chen, H. Kim, P. C. McIntyre, S. F. Bent, *Chem. Mater.* **2005**, *17*, 536.
[37] J. M. Castillo, M. Klos, K. Jacobs, M. Horsch, H. Hasse, *Langmuir* **2015**, *31*, 2630.
[38] A. Chandekar, S. K. Sengupta, J. E. Whitten, *Appl. Surf. Sci.* **2010**, *256*, 2742.

[39] L. Carbonell, C. M. Whelan, M. Kinsella, K. Maex, *Superlattices Microstruct.* **2004**, *36*, 149.
[40] M. M. Sung, K. Sung, C. G. Kim, S. S. Lee, Y. Kim, *J. Phys. Chem. B* **2000**, *104*, 2273.
[41] G. J. Kluth, M. M. Sung, R. Maboudian, *Langmuir* **1997**, *13*, 3775.
[42] S. Jeon, S. Bang, S. Lee, S. Kwon, W. Jeong, H. Jeon, H. J. Chang, H.-H. Park, *J. Electrochem. Soc.* **2008**, *155*, H738.
[43] A. Asyuda, S. Das, M. Zharnikov, *J. Phys. Chem. C* **2021**, *125*, 21754.
[44] D. Bobb-Semple, K. L. Nardi, N. Draeger, D. M. Hausmann, S. F. Bent, *Chem. Mater.* **2019**, *31*, 1635.
[45] W. L. Gladfelter, *Chem. Mater.* **1993**, *5*, 1372.
[46] T.-L. Liu, S. F. Bent, *Chem. Mater.* **2021**, *33*, 513.
[47] I. K. Oh, T. E. Sandoval, T.-L. Liu, N. E. Richey, S. F. Bent, *Chem. Mater.* **2021**, *33*, 3926.
[48] T. L. Liu, L. Zeng, K. L. Nardi, D. M. Hausmann, S. F. Bent, *Langmuir* **2021**, *37*, 11637.
[49] W. Volksen, R. D. Miller, G. Dubois, *Chem. Rev.* **2010**, *110*, 56.